ANS fluorescence: Potential to discriminate hydrophobic sites of proteins in solid states

Aytaj J. Guliyeva, Oktay K. Gasymov [*]

Laboratory of Structure, Dynamics and Functions of Biomolecules, Institute of Biophysics of ANAS, 117 Z. Khalilov, Baku, AZ1171, Azerbaijan

ARTICLE INFO

ABSTRACT

In the current study, ANS fluorescence was established as a powerful tool to study proteins in solid-state. Silk fibroin from *Bombyx mori* cocoons was used as a paradigm protein. ANS incorporated into the films of silk fibroin exhibits fluorescence with two-lifetime components that can be assigned to the patches and/or cavities with distinct hydrophobicities. Decay associated spectra (DAS) of ANS fluorescence from both sites could be fit to the single log-normal component indicating their homogeneity. ANS binding sites in the protein film are specific and could be saturated by ANS titration. ANS located in the binding site that exhibits the long-lifetime fluorescence is not accessible to the water molecules and its DAS stays homogeneously broadened upon hydration of the protein film. In contrast, ANS from the sites demonstrating the short-lifetime fluorescence is accessible to water molecules. In the hydrated films, solvent-induced fluctuations produce an ensemble of binding sites with similar characters. Therefore, upon hydration, the short-lifetime DAS becomes significantly red-shifted and inhomogeneously broadened. The similar spectral features have previously been observed for ANS complexed with globular proteins in solution. The data reveal the origin of the short-lifetime fluorescence component of ANS bound to the globular proteins in aqueous solution. Findings from this study indicate that ANS is applicable to characterize dehydrated as well as hydrated protein aggregates, amyloids relevant to amyloid diseases, such as Alzheimer's, Parkinson, and prion diseases.

1. Introduction

8-anilino-1-naphthalenesulfonic acid (ANS), as an extrinsic fluorescent probe is widely utilized to characterize proteins in various states [1]. In a molten globule state, enhancement of ANS fluorescence indicates that the hydrophobic clusters of proteins are exposed [2–5]. The time-resolved fluorescence of ANS bound to proteins provides a more detailed description of the hydrophobic clusters. Long- (10–15 ns) and short- (2–5 ns) lifetimes of ANS correspond to the solvent shielded and exposed hydrophobic clusters, respectively [5–10]. Fluorescent probes thioflavin T (ThT) and ANS are used together to study kinetics and mechanisms of amyloid fibril formations relevant to the serious diseases, such as Alzheimer's, Parkinson's, prion diseases, etc [11–15]. ANS fluorescence has also been used to study the pH- and urea-dependent structural transitions as well as to characterize the multiple binding sites of the proteins [16,17].

Mechanisms by which ANS contributes to fluorescence enhancement processes are broadly studied. ANS free in aqueous solution demonstrates a negligible fluorescence intensity with a maximum of around 540 nm. It has been suggested that both restricted mobility and hydrophobicity of the nearest environment of ANS contribute significantly to the blue shift of the fluorescence spectra and increased fluorescence intensity and lifetime. The application of steady-state fluorescence provides limited information about hydrophobic sites of the proteins. In the presence of multiple binding sites, the contribution of external hydrophobic sites exposed to solvent is masked by more intense fluorescence from buried sites. The time-resolved fluorescence of ANS offers a more detailed description of the hydrophobic sites associated with different degrees of solvent exposure.

ANS fluorescence depends on ion pairing with positively charged side chains, a variation of solvent polarity and viscosity [18–21]. Two distinct excited states contribute to the emission of ANS [22,23]. Non-polar (NP) state localized on the naphthalene moiety of ANS is the first step of the excitation event. NP state is the fluorescent state for ANS in hydrophobic solvents. The wavelength of fluorescence maximum of ANS from this state moderately depends on polarity. In polar solvents, NP state relaxes to form the intramolecular charge-transfer state (ICT), which is dynamically stabilized through molecular distortion and

---

solvent relaxation. Along with intermolecular electron transfer (ET), ionization and subsequent electron salvation were also detected in the aqueous solution of ANS. ET is considered to be a major quenching mechanism for ANS fluorescence yielding a very low quantum yield [22, 23]. Fluorescence of ANS in polar solvents is attributed to the emission from charge transfer state (CT).

Until now, however, ANS has been applied only to characterize the various protein states in solution. No efforts have been made to show the feasibility of ANS to characterize protein in solid states. In this study, ANS was incorporated into silk fibroin (SF) films to characterize the hydrophobic cluster of the protein in solid-state. The time-resolved fluorescence of ANS incorporated into the SF film indicates that it has the potential to characterize protein sites with different hydrophobicities linked to the distinct fluorescence lifetimes. Partial hydration of the SF films further discriminates hydrophobic sites by accessibility to the water molecules. The results unambiguously reveal the origin of the protein sites where ANS fluorescence shows inhomogeneously broadened spectra with the lifetimes of about 2–5 ns. These hydration induced spectral features have also been demonstrated for globular proteins in solution. SF was used as a paradigm protein. Steady-state and time-resolved fluorescence can be utilized with ANS to characterize other proteins in fiber, film, and dehydrated amyloid fibril forms. The application by using the ANS fluorescence can also be used to monitor the hydration dynamics of amyloid fibrils that are relevant to neurodegenerative disease propagation.

2. Materials and methods

2.1. Preparation of aqueous solution of silk fibroin

Silk cocoons from the silkworm of *Bombyx mori* were used to obtain silk fibroin using a widely employed degumming procedure [24,25]. Silk cocoons cut into small pieces boiled for 30 min in 0.02 M Na_2CO_3 (Fisher Sci.) and then rinsed extensively with deionized water to remove sericin. The air-dried SF was dissolved in 9.5 M LiBr (Sigma-Aldrich) solution and then dialyzed (molecular weight cut-off 10 kDa) against deionized water 48 h at 4 °C. Then the silk solution was centrifuged for 10 min at 9000 rpm, and the supernatant was collected and stored at 4 °C. The concentration of the stock solution of SF was determined by spectrophotometer using $\varepsilon_{275nm} = 1.064$ cm^{-1} $(mg/ml)^{-1}$ [26]. The molar concentration of the solution was calculated using 390 kDa for the molecular weight of SF. The final concentration of the stock solution of SF was determined to be 95 μM.

2.2. Preparation of ANS incorporated films of silk fibroin

The stock solution of ANS was prepared with deionized water and its concentration was determined using the molar extinction coefficient of $\varepsilon_{350nm} = 4950$ $M^{-1}cm^{-1}$ (provided by Sigma-Aldrich). The solution of SF (95 μM) was used to prepare the mixtures with various molar ratios of SF:ANS (1:0.13, 1:0.35, 1:0.72, 1:0.87, 1:1). The films were obtained by slow evaporation of the mixture solutions on polystyrene substrates. The formation of ANS aggregates is not expected in the films with SF:ANS above shown ratios. Aggregate formation of the ligand (rhodamine 6G) in the SF matrix was examined previously. It has been shown that the ligand binding to the protein prevents aggregate formation even in mM concentrations of the ligand [25]. Besides, the lifetimes of DAS components of ANS fluorescence are not changed much in the films with various SF:ANS ratios. Usually, aggregate formations of the chromophores result in decreased fluorescence lifetimes.

Hydration of the films was performed using two quartz plates sealed with a spacer. The film was placed in the vertical position between the quartz plates. The bottom of the quartz plates was filled with water that did not touch the film. The system was left to equilibrate for one day. The hydration value was determined immediately after the experiment by weight.

2.3. Absorption spectroscopy

UV absorption spectra of fibroin solutions and films with various SF: ANS ratios were measured using Shimadzu UV-2700 spectrophotometer. Spectral bandwidth was set to1.0 nm.

2.4. Steady-state and time-resolved fluorescence spectroscopy

Steady-state and time-resolved fluorescence were recorded using a spectrofluorometer FluoTime 300 (PicoQuant, Germany). The steady-state measurements were performed in front-face mode using an excitation wavelength of 375 nm. Bandwidths for excitation and emission were 3 nm. In the time-resolved experiments, a picosecond laser with a wavelength of 375 nm was used for excitation. The emission bandwidth was 2.5 nm.

2.5. Construction of decay-associated spectra (DAS)

To construct DAS for various SF:ANS films, the ANS fluorescence decay measurements were performed for the wavelengths across the emission spectra with a 5 nm interval. The emission intensity was measured with a front-face setup. The instrument response function (IRF) was determined by measuring scattered light from pristine SF film. The intensity decay data were analyzed using the software supplied with the PicoQuant instrument. For a multiexponential decay law:

$$I(t) = \sum a_i \exp(-t/\tau_i)$$

where I, a_i and τ_i are fluorescence intensity, the normalized pre-exponential factors, and decay time, respectively. The fractional fluorescence intensity of each component is defined as $f_i = a_i\tau_i / \sum a_j\tau_j$.

Decay-associated spectra were assembled using global multi-exponential decay analysis across the emission spectra of the films with various SF:ANS ratios [27].

$$I(\lambda, t) = \sum a_i(\lambda)\exp(-t/\tau_i)$$

Then $a_i(\lambda)$ values were used to construct the DAS for each global τ_i parameter

$$I_i(\lambda) = \frac{a_i(\lambda)\tau_i I(\lambda)}{\sum a_j(\lambda)\tau_j} = f_i(\lambda)I(\lambda)$$

DAS components were fit to the bi-parametric log-normal function. The parameters specific for ANS fluorescence were established previously [6].

3. Results and discussion

3.1. The absorption spectra of ANS bound to proteins in film and solution states show similar features

Properties of the ANS absorption band positioned in the longer wavelength side of the spectrum have been studied in solvents with various polarities. This band is composite and can be characterized by the superposition of two spectra with the absorption maximum of about 375 nm and 355 nm. The substitution of solvent from water to dioxane leads to an increase of the ratio of intensities R = $\lambda_{max}(1)/\lambda_{max}(2)$ (~375 nm and ~355 nm, respectively) from 0.90 to 1.17 [22]. In aqueous solution, the absorption band of ANS can be characterized by two Gaussian components with $\lambda_{max}(1) = 377.3$ nm and $\lambda_{max}(2) = 338.3$ nm (Supplementary Fig. 1). The inclusion of ANS molecules into SF films exhibits a significant red-shift for both absorption bands (377.3 nm–385 nm and 338.3 nm–348.9 nm). The ratio of intensities $\lambda_{max}(1)/\lambda_{max}(2)$ increases from 0.95 to 1.20, which closely matches the changes observed from the substitution of water with dioxane (Supplementary Fig. 1). Almost identical spectral changes have been observed between ANS free

and bound to the protein in solution [28]. Observed changes in the absorption spectra are most likely to have resulted from the modification of the electron density distribution of ANS molecules. This indicates a complex formation between ANS molecules and some groups of protein molecules. ANS binding characteristics in the film are strikingly similar to the binding in aqueous solution. ANS in the SF film can be described as ANS molecules bound to binding sites of the protein. Below we show the evidence for two distinct specific binding sites for ANS binding in the SF film.

3.2. Steady-state fluorescence and DAS components of ANS

ANS fluorescence spectra in various solvents can be satisfactorily characterized by the single log-normal component indicating the homogeneous nature of the ANS environment [6]. A single log-normal component, also named as an elementary component, is characterized by two parameters, wavelength of fluorescence maximum and scaling factor. Other parameters of the log-normal function are fixed and satisfactory for all ANS fluorescence spectra in different solvents [6]. The log-normal function was used to characterize the DAS components of ANS fluorescence in the films with different SF:ANS ratios (Fig. 1). Three lifetimes were necessary for satisfactory fitting in the global analysis. Fig. 1A–E shows the steady-state fluorescence spectra and resolved DAS components for ANS fluorescence in the representative SF: ANS films with ratios of 1:0.13, 1:0.35, 1:0.72, 1:0.87 and 1:1, respectively. As an example, the global triple-exponential decay fits are shown for the SF:ANS (1:0.35) film at various wavelengths (Fig. 1F). The dissimilar contributions of the fast decay components are evident at the beginning of the decay curves. The decay curves for selected wavelengths are plotted separately for better judgment (Supplementary Fig. 2). All films with different SF:ANS ratios show a similar set of lifetimes (Fig. 2). To test the validity of the triple-exponential decay model, a representative ANS fluorescence decay was also analyzed by a model-free maximum entropy method (MEM). In the MEM, a series of 200 exponentials, logarithmically spaced lifetimes and variable pre-exponential terms were used. The goal of the fitting procedure was to have the minimized χ^2 and maximized Shannon–Jaynes entropy function [29]. The results of the ANS fluorescence decay analysis by the MEM are shown in Supplementary Fig. 3. The lifetime components from
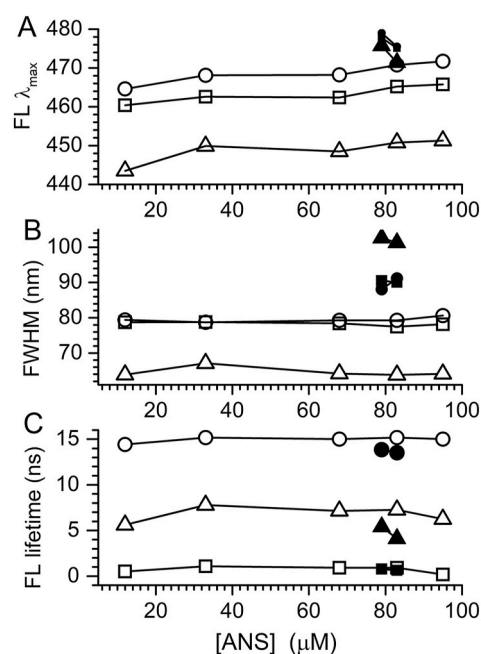

Fig. 2. The steady-state and time-resolved fluorescence parameters of ANS in the films with various SF:ANS ratios. The concentration of ANS indicates their corresponding values in the solution from which films were made. Actual concentrations are about ×40 as estimated previously. Open squares, triangles and circles represent the parameters of the DAS corresponding to the very short-, short- and long lifetimes shown in (C). Solid symbols show the parameters of the DAS of the hydrated samples of the corresponding counterparts.

the MEM analysis can be grouped into three classes with the maximum values of 1.0 ns, 8.6 ns and 15.6 ns. These data are in good agreement with the fluorescence lifetimes obtained from the triple-exponential decay model (1.1 ns, 7.8 ns, 15.2 ns). Thus, MEM analysis validates the use of the triple-exponential decay model for ANS fluorescence decay and DAS in the different SF:ANS films.

The steady-state fluorescence spectra of ANS in various SF:ANS are inhomogeneously broadened and, therefore, could not be fit to the single
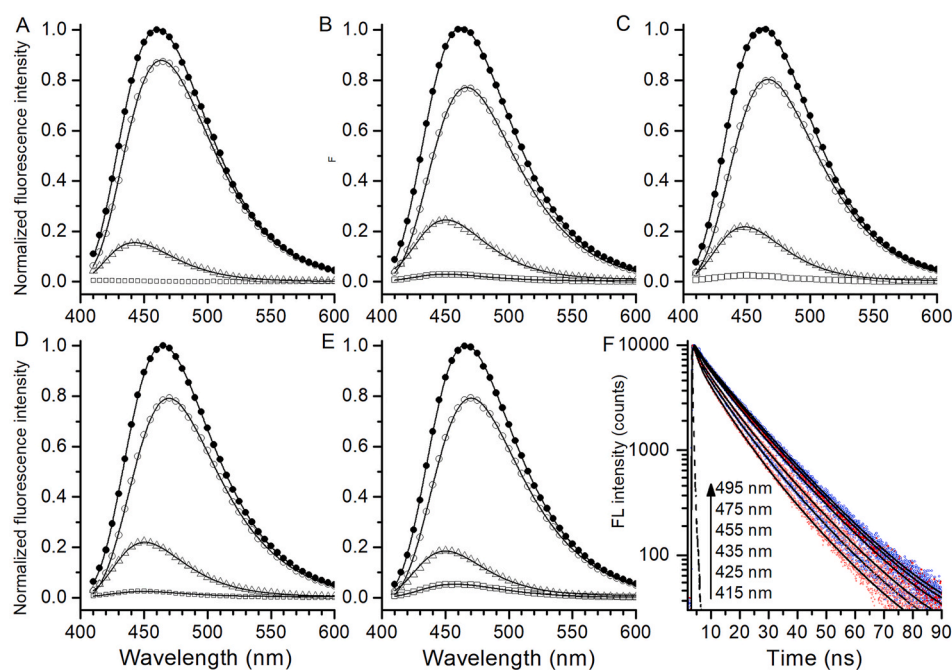

Fig. 1. Steady-state emission spectra and DAS components of ANS incorporated into SF films at various SF:ANS ratios. (A)–(E) represents SF:ANS films with ratios of 1:0.13, 1:0.35, 1:0.72, 1:0.87 and 1:1, respectively. Solid circles represent steady-state fluorescence spectra. Open square, triangle and circles denote DAS components for very short- (0.19 ns- 1.08 ns), short- (5.62 ns- 7.79 ns) and long (14.41 ns- 15.18 ns) lifetime components. The solid lines of DAS components show the best fit to the single log-normal function with parameters specific for ANS. (F) Fluorescence intensity decay curves of ANS in SF:ANS (1:0.35) film at various wavelengths. Circles are experimental data points. The dashed line is an instrument response function. Solid curves denote the best fit for global triple-exponential decay.

log-normal component. As an example, a single and double log-normal component fit of the ANS fluorescence spectrum in the film SF:ANS (1:0.35) is shown in Supplementary Fig. 4. At least two log-normal components are required for satisfactory fitting of the spectrum. The values of the wavelength of fluorescence maximum obtained from the log-normal fit do not match that of DAS components (Fig. 1B and Supplementary Fig. 4.). Therefore, the multicomponent log-normal fit is not adequate to resolve a DAS component. However, it is valuable to show the presence of the inhomogeneous broadening in the ANS fluorescence spectra.

Individual DAS of ANS fluorescence in the films with various SF:ANS ratios can be satisfactorily fit the single log-normal component. This is in contrast to the data observed for ANS bound to the protein in solution [6]. ANS bound to apo-tear lipocalin (apo-TL) and its mutant apo-G59W shows two DAS components relatively short (4.09 and 4.64 ns) and the longer lifetime (17.33 and 15.82 ns) components, respectively [6]. In both cases, relatively short lifetime DAS could not be fit to a single log-normal component. However, long lifetime DAS of ANS-apoG59W, but not ANS-apoTL, can be satisfactorily fit a single log-normal component. It has been concluded that the heterogeneous nature of ANS binding sites necessitates the fitting of the DAS to double log-normal components. Interestingly, both short- and long lifetime DAS components of ANS fluorescence in the films with various SF:ANS ratios can be characterized by single log-normal components. This indicates that in the solid protein film, ANS is bound to the sites with two different hydrophobicities, but environments of the binding sites in both cases are homogeneous.

The steady-state spectra and the resolved DAS components of ANS fluorescence in the films with various SF:ANS ratios reveal the nature of ANS-SF interaction. Despite significant differences in wavelengths of fluorescence maxima of between DAS, the same DAS component exhibits a minor variation at different ANS concentration (Fig. 2). The same statement is also true for the lifetime components of DAS. Data indicate that even in solid-state ANS binding sites of SF are distinct and specific. The increased concentrations of ANS saturate the specific binding sites (Fig. 2 and Supplementary Fig. 5). Thus, as in solution studies, ligand (ANS)- protein (SF) interaction in solid states can be described in similar terms, saturations of specific binding sites. Compared to solution studies, SF in solid-state assumes much less conformational states that are supported by homogeneous DAS components of ANS fluorescence.

ANS bound to proteins in solution shows blue-shifted fluorescence maxima, the increase fluorescence intensity and lifetimes that are attributed to the hydrophobicity of a protein site and restriction of mobility of ANS. Incorporation of ANS into the solid film of SF eliminates one of these factors, i.e., mobility. In the solid protein film, the mobility of all sites is significantly restricted. Therefore, it is expected that the lifetimes of ANS incorporated into the solid protein films will be mainly influenced by the hydrophobicity of the sites. ANS in the SF:ANS films shows fluorescence with three lifetimes, very short- (0.19 ns- 1.08 ns), short- (5.62 ns- 7.79 ns) and long- (14.41 ns- 15.18 ns). Very short-lifetimes are associated with very low fluorescence intensities. Therefore, DAS and the lifetimes for these components were not consistent in the films with various SF:ANS ratios. The short- and long-lifetime components could be compared to that of ANS bound to TL and beta-lactoglobulin in solution [6,9,10]. The long-lifetime of ANS in the SF:ANS films (14.41 ns- 15.18 ns) are very similar to that of ANS-TL and ANS-G59W (17.33 ns and 15.82 ns, respectively, and ANS-BLG (~14 ns) complexes. Thus, long-lifetimes of ANS report high hydrophobicity and restricted mobility in both incorporated into the protein films and complexed with globular proteins in solutions. The situation is different with the short-lifetimes. In the solid protein matrix, the short-lifetimes of ANS fluorescence are in a range of 5.62 ns – 7.79 ns. It can be compared with the short-lifetimes of ANS-TL and ANS-G59W (4.09 ns and 4.46 ns, respectively) and ANS-BLG (~3 ns) complexes in solution [6,9,10]. Short-lifetimes of ANS in the SF:ANS films are appreciably higher than

that of the proteins in solution (Figs. 1 and 2). This fact can be rationalized by the solvation of the ANS binding sites responsible for short fluorescence lifetimes in solution. ANS is expected to have relatively higher mobility in the solvated states.

To test this hypothesis we performed the experiments with the hydrated SF:ANS films. Fig. 3 shows the steady-state and DAS component of ANS fluorescence in the SF:ANS (1:0.83) film without and with hydration. The hydrated samples demonstrate red-shifted steady-state and DAS components. However, the shifts are not uniform among the DAS components. The DAS component with long-lifetime shows the smallest shift, the spectrum of which could be fit to the single log-normal component (Figs. 2 and 3). Hydration of the film induces a slight decrease (~9%) of the fluorescence lifetime, from 15.18 ns to 13.84 ns. Consequently, it can be concluded that the hydrophobic sites responsible for long-lifetimes of ANS fluorescence are not solvated and homogeneous. In contrast, upon the hydration, the DAS component with short-lifetime shows a large red-shift and inhomogeneous broadening (Figs. 2 and 3). As a result, the short-lifetime DAS requires at least two log-normal components for satisfactory fitting (Fig. 3). Compared to the long-lifetime, upon hydration of the film the short-lifetime of ANS fluorescence exhibits a considerable (~26%) decrease, from 7.27 ns to 5.4 ns. All parameters, spectral FWHM, lifetime and wavelength of fluorescence maximum, of ANS fluorescence in the SF film corresponding short-lifetime DAS upon hydration become similar to that of ANS complexed with globular proteins in solution. The inhomogeneous broadening of the short-lifetime DAS indicates that hydration generates multiple conformational states. In the protein film, hydration disrupts homogeneously distributed ANS binding sites responsible for the short-lifetime DAS and fluctuation induced by hydration enables it to sample an ensemble of patches and/or cavities with similar hydrophobicity. Slow rate desiccation of the films removes hydration related dynamics and an ensemble of substates becomes trapped into the energetically minimum state. ANS incorporated into these states yields homogeneously broadened DAS (short-lifetime component).

Thus, the results observed for the partially hydrated (45%) films reveal the origin of the inhomogeneously broadened DAS with lifetimes of about 3–5 ns observed in solution studies. It is important to notice that binding sites with different hydrophobicities revealed in the SF films by ANS fluorescence are specific. Indeed, titration of SF films with various concentrations of ANS exhibits saturation behavior for the steady-state intensity and DAS of short- and long-lifetimes (Supplementary Fig. 5). The DAS component for very short-lifetime does not saturate. Most likely, this fluorescence originates from ANS molecules localized in void volumes of the protein films, analogous to free ANS in solution.

The relationship between the wavelengths of fluorescence maximum and lifetimes of ANS complexed with various proteins is revealing (Fig. 4). It is evident that there is a linear relationship between the wavelengths of fluorescence maximum and lifetimes for both short- and long lifetimes in the desiccated SF films. However, in the solution and hydrated protein films, only long lifetime components follow that trend. The short lifetimes of ANS fluorescence do not depend on the wavelengths of fluorescence maximum values in the hydrated SF film and globular proteins in solution.

4. Conclusion

Thus, ANS has the potential to characterize proteins in various solid states to reveal the hydrophobic sites with distinct features. ANS in the solvent accessible sites exhibits relatively short-lifetime DAS that in hydrated states becomes very similar to that of ANS-globular protein complexes in solution. ANS in binding sites characterized by long lifetime DAS is not solvent accessible. ANS fluorescence properties revealed in the protein films indicate that it can be used to characterize dehydrated as well as hydrated protein aggregates, amyloids relevant to the Alzheimer's, Parkinson, and prion diseases.
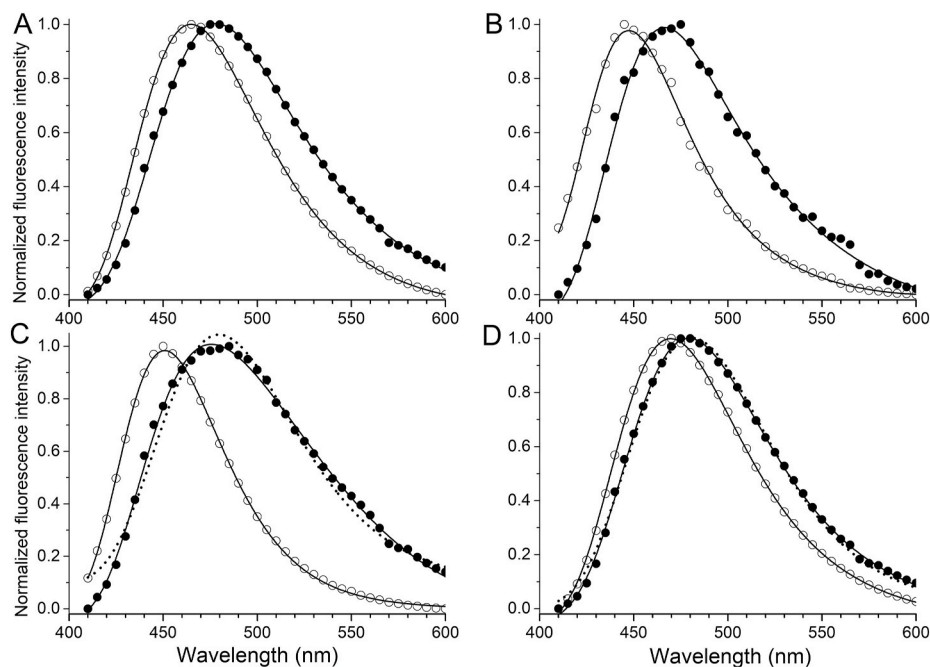
Fig. 3. The influence of hydration (45%) on the DAS component of ANS in the film with SF:ANS (1:0.83). (A), the steady-state spectra of ANS in the film with desiccated (open circles) and hydrated (solid circles) states. (B), (C) and (D) represent very short-, short- and long lifetime DAS components of ANS in the film with desiccated (open circles) and hydrated states (solid circles). Solid lines in (C) and (D) represent a single log-normal fit for the film with desiccated forms. (C) and (D) for the hydrated state, dashed- and solid lines show single- and double log-normal component fitting.
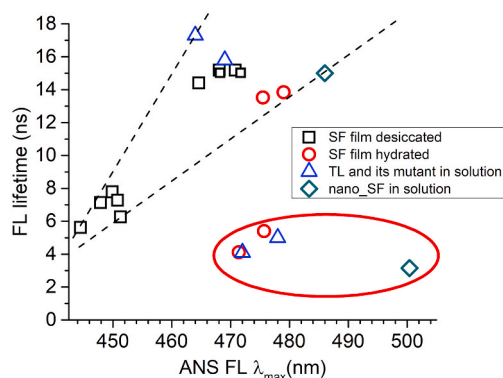

Fig. 4. Fluorescence lifetimes versus fluorescence maximum wavelength for ANS in different conditions. The lifetimes represent the resolved DAS components. Data for nano-SF are from unpublished data. The red ellipse highlights the region for short-lifetime DAS components in solution. (For interpretation of the references to colour in this figure legend, the reader is referred to the Web version of this article.)

Funding

Declaration of competing interest

The authors declare that there is no conflict of interest.

Acknowledgment

None.

Appendix A. Supplementary data

Supplementary data related to this article can be found at https://doi.org/10.1016/j.bbrep.2020.100843.

References

[1] A. Hawe, M. Sutter, W. Jiskoot, Extrinsic fluorescent dyes as tools for protein characterization, Pharm. Res. 25 (2008) 1487–1499, https://doi.org/10.1007/s11095-007-9516-9.

[2] V.E. Bychkova, R. Berni, G.L. Rossi, V.P. Kutyshenko, O.B. Ptitsyn, Retinol-binding protein is in the molten globule state at low pH, Biochemistry 31 (1992) 7566–7571, https://doi.org/10.1021/bi00148a018.

[3] O.K. Gasymov, A.R. Abduragimov, B.J. Glasgow, Molten globule state of tear lipocalin: ANS binding restores tertiary interactions, Biochem. Biophys. Res. Commun. 357 (2007) 499–504, https://doi.org/10.1016/j.bbrc.2007.03.186.

[4] E. Bismuto, G. Irace, I. Sirangelo, E. Gratton, Pressure-induced perturbation of ANS-apomyoglobin complex: frequency domain fluorescence studies on native and acidic compact states, Protein Sci. 5 (2008) 121–126, https://doi.org/10.1002/pro.5560050115.

[5] K. Singh, I. Hussain, V. Mishra, M.S. Akhtar, New insight on 8-anilino-1-naphthalene sulfonic acid interaction with TgFNR for hydrophobic exposure analysis, Int. J. Biol. Macromol. 122 (2019) 636–643, https://doi.org/10.1016/j.ijbiomac.2018.10.208.

[6] O.K. Gasymov, A.R. Abduragimov, B.J. Glasgow, Characterization of fluorescence of ANS-tear lipocalin complex: evidence for multiple-binding modes, Photochem. Photobiol. 83 (2007) 1405–1414, https://doi.org/10.1111/j.1751-1097.2007.00180.x.

[7] E. Gabellieri, G.B. Strambini, ANS fluorescence detects widespread perturbations of protein tertiary structure in ice, Biophys. J. 90 (2006) 3239–3245, https://doi.org/10.1529/biophysj.105.074948.

[8] W.G. Gonzalez, J. Miksovska, Application of ANS fluorescent probes to identify hydrophobic sites on the surface of DREAM, Biochim. Biophys. Acta Protein Proteonomics 1844 (2014) 1472–1480, https://doi.org/10.1016/j.bbapap.2014.05.004.

[9] M. Collini, L. D'Alfonso, G. Baldini, New insight on β-lactoglobulin binding sites by 1-anilinonaphthalene-8-sulfonate fluorescence decay, Protein Sci. 9 (2000) 1968–1974, https://doi.org/10.1110/ps.9.10.1968.

[10] L. D'Alfonso, M. Collini, G. Baldini, Evidence of heterogeneous 1-anilinonaphthalene-8-sulfonate binding to β-lactoglobulin from fluorescence spectroscopy, Biochim. Biophys. Acta Protein Struct. Mol. Enzymol. 1432 (1999) 194–202, https://doi.org/10.1016/S0167-4838(99)00105-3.

[11] A. Ghahghaei, S. Shahraki, Inhibitory effect of β-casein on the amyloid fibril formation of aβ1-40 associated with Alzheimer's disease, Int. J. Pept. Res. Therapeut. 22 (2016) 23–29, https://doi.org/10.1007/s10989-015-9482-8.

[12] S. Lee, M.C. Choi, K. Al Adem, S. Lukman, T.Y. Kim, Aggregation and cellular toxicity of pathogenic or non-pathogenic proteins, Sci. Rep. 10 (2020) 1–14, https://doi.org/10.1038/s41598-020-62062-3.

[13] P. Patel, K. Parmar, D. Patel, S. Kumar, M. Trivedi, M. Das, Inhibition of amyloid fibril formation of lysozyme by ascorbic acid and a probable mechanism of action, Int. J. Biol. Macromol. 114 (2018) 666–678, https://doi.org/10.1016/j.ijbiomac.2018.03.152.

[14] R. Khurana, J.R. Gillespie, A. Talapatra, L.J. Minert, C. Ionescu-Zanetti, I. Millett, et al., Partially folded intermediates as critical precursors of light chain amyloid fibrils and amorphous aggregates, Biochemistry 40 (2001) 3525–3535, https://doi.org/10.1021/bi001782b.

[15] S. Kumar, K. Tepper, S. Kaniyappan, J. Biernat, S. Wegmann, E.M. Mandelkow, et al., Stages and conformations of the Tau repeat domain during aggregation and its effect on neuronal toxicity, J. Biol. Chem. 289 (2014) 20318–20332, https://doi.org/10.1074/jbc.M114.554725.

[16] O.K. Gasymov, A.R. Abduragimov, B.J. Glasgow, Evidence for internal and external binding sites on human tear lipocalin, Arch. Biochem. Biophys. 468 (2007) 15–21, https://doi.org/10.1016/j.abb.2007.09.011.

[17] M. Collini, L. D'Alfonso, H. Molinari, L. Ragona, M. Catalano, G. Baldini, Competitive binding of fatty acids and the fluorescent probe 1-8-anilinonaphthalene sulfonate to bovine β-lactoglobulin, Protein Sci. 12 (2003) 1596–1603, https://doi.org/10.1110/ps.0304403.

[18] D. Matulis, R. Lovrien, 1-Anilino-8-naphthalene sulfonate anion-protein binding depends primarily on ion pair formation, Biophys. J. 74 (1998) 422–429, https://doi.org/10.1016/S0006-3495(98)77799-9.

[19] J.J. Ory, L.J. Banaszak, Studies of the ligand binding reaction of adipocyte lipid binding protein using the fluorescent probe 1, 8-anilinonaphthalene-8-sulfonate, Biophys. J. 77 (1999) 1107–1116, https://doi.org/10.1016/S0006-3495(99)76961-4.

[20] A. Lartigue, A. Gruez, S. Spinelli, S. Rivière, R. Brossut, M. Tegoni, et al., The crystal structure of a cockroach pheromone-binding protein suggests a new ligand binding and release mechanism, J. Biol. Chem. 278 (2003) 30213–30218, https://doi.org/10.1074/jbc.M304688200.

[21] O.K. Gasymov, B.J. Glasgow, ANS fluorescence: potential to augment the identification of the external binding sites of proteins, Biochim. Biophys. Acta Protein Proteonomics 1774 (2007) 403–411, https://doi.org/10.1016/j.bbapap.2007.01.002.

[22] E.M. Kosower, H. Kanety, Intramolecular donor-acceptor systems. 10. Multiple fluorescences from 8-(phenylamino)-1 -naphthalenesulfonates, J. Am. Chem. Soc. 105 (1983) 6236–6243, https://doi.org/10.1021/ja00358a008.

[23] E.M. Kosower, D. Huppert, Excited state electron and proton transfers, Annu. Rev. Phys. Chem. 37 (1986) 127–156, https://doi.org/10.1146/annurev.pc.37.100186.001015.

[24] W. Huang, S. Ling, C. Li, F.G. Omenetto, D.L. Kaplan, Silkworm silk-based materials and devices generated using bio-nanotechnology, Chem. Soc. Rev. 47 (2018) 6486–6504, https://doi.org/10.1039/c8cs00187a.

[25] O.K. Gasymov, C. Botta, L. Ragona, A.J. Guliyeva, H. Molinari, Silk fibroin-based films enhance rhodamine 6G emission in the solid state: a chemical–physical analysis of their interactions for the design of highly emissive biomaterials, Macromol. Chem. Phys. 220 (2019), https://doi.org/10.1002/macp.201800460.

[26] L. Ragona, O. Gasymov, A.J. Guliyeva, R.B. Aslanov, S. Zanzoni, C. Botta, et al., Rhodamine binds to silk fibroin and inhibits its self-aggregation, Biochim. Biophys. Acta Protein Proteonomics 1866 (2018) 661–667, https://doi.org/10.1016/j.bbapap.2018.03.009.

[27] J.R. Lakowicz, Principles of Fluorescence Spectroscopy, Third, Springer, New York, 2006.

[28] I.M. Kuznetsova, A.I. Sulatskaya, O.I. Povarova, K.K. Turoverov, Reevaluation of ans binding to human and bovine serum albumins: key role of equilibrium microdialysis in ligand - receptor binding characterization, PloS One 7 (2012) 1–9, https://doi.org/10.1371/journal.pone.0040845.

[29] A.K. Livesey, J.C. Brochon, Analyzing the distribution of decay constants in pulse-fluorimetry using the maximum entropy method, Biophys. J. 52 (1987) 693–706, https://doi.org/10.1016/S0006-3495(87)83264-2.